Effects of Infiltration Characteristics on Spatial-Temporal Evolution of Stability of an Interstate Highway Embankment

Eric Hinds[1]; Ning Lu, F.ASCE[2]; Benjamin Mirus[3]; and Alexandra Wayllace, A.M.ASCE[4]

Abstract: Infiltration-induced landslides are among the most common natural disasters threatening modern civilization, but conventional methods for studying the triggering mechanisms and predicting the occurrence of these slides are limited by incomplete consideration of underlying physical processes and the lack of precision inherent in limit-equilibrium analyses. To address this problem, the spatial-temporal evolution of failure is investigated in a seasonally unstable section of an interstate highway embankment, known as the Straight Creek landslide, Colorado. The study includes multiyear site investigation, monitoring, and numerical simulation using a rigorous hydromechanical framework along with a field of local factor of safety method. The sensitivity of episodic landslide reactivation to infiltration characteristics is evaluated. Results indicate that annual cumulative snowmelt infiltration, which typically accounts for approximately 75% of total annual cumulative infiltration and occurs over a short period in the spring, has the most substantial impact on slide activation. The rate of snowmelt infiltration varies independently of annual cumulative snowmelt infiltration and cumulative infiltration in the previous year, but still affects antecedent soil-moisture conditions at the onset of snowmelt infiltration and therefore also the level of slide activation. These findings are used to establish specific thresholds for exacerbated slide movement using annual snowpack accumulation, forecasted snowmelt rate, and the previous year's snowmelt, an approach that may be applied for predicting movement at this and other recurring or potential slide sites.
DOI: 10.1061/(ASCE)GT.1943-5606.0002127.

Author keywords: Landslide initiation; Sensitivity analysis; Field monitoring; Numerical simulation; Local factor of safety; Slope instability threshold.

Introduction

Landslide occurrence is controlled by slope geometry, subsurface material properties, and trigger mechanisms, which include seismic activity, volcanism, erosion, construction and mining activity, and infiltration (Lu and Godt 2013). Of the most destructive landslides worldwide in the last century, half are believed to be infiltration-induced (Sidle and Ochiai 2006). Existing methods for predicting slope failure under infiltration conditions are typically indirect (i.e., based solely on depth of surficial deposits), empirical (rainfall intensity-duration curves), or based on classical soil mechanics and limit-equilibrium methods, which do not always capture the relatively small and often localized changes in effective stress or suction stress that frequently initiate infiltration-related landslides. A physics-based approach that explicitly considers transient unsaturated subsurface flow and mechanics and localized stress evolution has the potential to improve prediction of slide occurrence through deeper understanding of underlying physical processes. A scientific challenge is thus understanding what are the controls of the recurring landslides in terms of infiltration characteristics?

The Straight Creek landslide, along an embankment of Interstate-70 (I-70) in the Colorado Rocky Mountains, is the subject of this investigation. It is located in Summit County, Colorado, approximately 80 km (50 mi) west of Denver (Fig. 1). The landslide is a recurring failure that continually crosses between stable and unstable states, experiencing at least some movement every year. Whereas many landslides experience a specific failure one time, this recurring slide fails in essentially the same mode every year, although to varying degrees. This allows a sensitivity analysis of the embankment's stability to various factors using field data, in addition to numerical and analytic modeling. This case study develops an approach to quantify the controls on the activation length of recurring infiltration-triggered landslides and thereby identify physics-based thresholds for reactivation. The resulting insights contribute to understanding the specific trigger mechanisms and levels of risk for other similar sites.

The embankment affected by the Straight Creek slide was constructed in the late 1960s from excavated material, or cuttings, from the nearby Continental Divide–crossing Eisenhower-Johnson Memorial Tunnels (Robinson & Associates 1971). Slides in the surrounding hillslopes were triggered by slope-cutting operations, leading to the first geotechnical investigation of the area by Robinson & Associates in 1969. This investigation provided information on the local geology and scattered water table position measurements. In 1973, a bulge appeared in the eastbound lanes; sometime in the mid-1970s, the bulging turned to downslope

[1]Graduate Research Assistant, Dept. of Civil and Environmental Engineering, Colorado School of Mines, Golden, CO 80401. Email: ehinds@mines.edu

[2]Professor, Dept. of Civil and Environmental Engineering, Colorado School of Mines, Golden, CO 80401 (corresponding author). ORCID: https://orcid.org/0000-0003-1753-129X. Email: ninglu@mines.edu

[3]Research Geologist, Landslide Hazards Program, US Geological Survey, Denver, CO 80225. ORCID: https://orcid.org/0000-0001-5550-014X. Email: bbmirus@usgs.gov

[4]Teaching Associate Professor, Dept. of Civil and Environmental Engineering, Colorado School of Mines, Golden, CO 80401. Email: awayllac@mines.edu

Note. This manuscript was submitted on June 15, 2018; approved on April 17, 2019; published online on July 11, 2019. Discussion period open until December 11, 2019; separate discussions must be submitted for individual papers. This paper is part of the ***Journal of Geotechnical and Geoenvironmental Engineering***, © ASCE, ISSN 1090-0241.

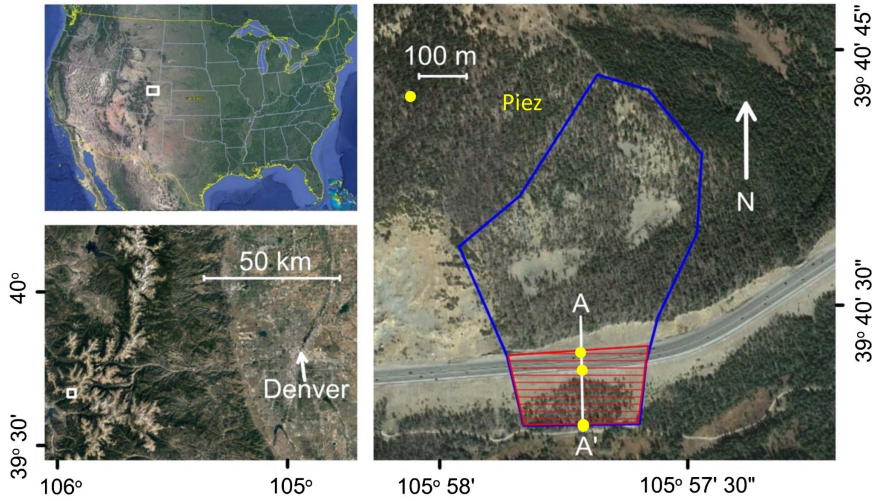

Fig. 1. Straight Creek slide location and extents. Approximate slide area is shaded, and approximate watershed area is outlined above the shaded area. Transect indicated by AA-–^{A} / is shown in Fig. 2. (Map data © 2018 Google Earth.)

movement, causing subsidence of the highway surface. What was then the Colorado Department of Highways [now the Colorado Department of Transportation (CDOT)] assumed that the subsidence was due to settlement of the embankment material and addressed it with asphalt capping to maintain a level traffic surface. However, the movement did not stop. In 1996, CDOT commissioned an investigation by Kumar & Associates into the cause of subsidence and potential remediation strategies. This investigation provided further geological characterization and the identification of a sheared zone below the embankment that indicated an ongoing slide failure (Kumar & Associates 1997).

CDOT initiated an investigation in partnership with researchers at the Colorado School of Mines (CSM) and the US Geological Survey Landslide Hazards Program (USGS-LHP) in 2010. This investigation has progressed in three successive phases. Phase I consisted of mapping the spatial extents of the slide, drilling three boreholes to further characterize subsurface materials and their distribution, installing piezometers in all three boreholes to monitor groundwater levels, installing inclinometers below both shoulders of the highway to monitor slide movement, and developing a conceptual model of the site's seasonal hydrology whereby the rapid melting of accumulated snowpack causes destabilizing increases in pore pressure. The detection of an unusually pronounced spike in springtime and summertime groundwater levels below the upslope, westbound shoulder (Lu and Wayllace 2011; Wayllace et al. 2012) prompted the installation of an additional piezometer on the slope above the highway in Phase II of the investigation. This second phase also encompassed the gathering of precipitation and snowpack data, which along with the piezometer data were used to constrain several numerical models that confirmed and refined the conceptual model of seasonal hydrology and its effects on slope stability.

This work, which reports on Phase III of the investigation, addresses the spatial-temporal evolution of instability in the Straight Creek slide and its sensitivity to infiltration characteristics by using field data on precipitation, snowpack, and groundwater conditions, along with coupled hydromechanical numerical modeling. The questions to be addressed are as follows:

- How sensitive is embankment stability to annual variability in infiltration characteristics, including the total annual cumulative infiltration from snowmelt and rainfall, the rate at which that infiltration occurs, and variability in its timing?
- Can infiltration conditions in previous years affect site hydrology and embankment stability in a given year?
- Can infiltration characteristics be used to predict instability?

Study Site Characterization and Instrumentation

The section of I-70 affected by the Straight Creek landslide is at an elevation of approximately 3,252 m (10,670 ft) above sea level and is situated on a south-facing slope with a roughly 30° inclination. The slide mass is approximately 175 m wide and 123 m long (Lu and Wayllace 2011; Fig. 1). The site is within the Williams Fork Mountains, which are primarily composed of metasedimentary gneiss, schist, and pegmatite bedrock. Exposure to hydrologic conditions, including infiltration and freeze-thaw cycles, has resulted in a thick layer of weathered bedrock overlain by thin colluvial deposits (Lovering 1935). Mountain conifers and aspens cover most of the area below 3,597 m, although there are some natural rock outcroppings and bare faces created by cutting.

The two-dimensional distribution of materials along a centerline transect through the slide (Fig. 2) was derived from borehole logs from past investigations (Lovering 1935; Robinson & Associates 1971; Kumar & Associates 1997; Thunder 2016) and drilling conducted during the current study. Hydromechanical properties are

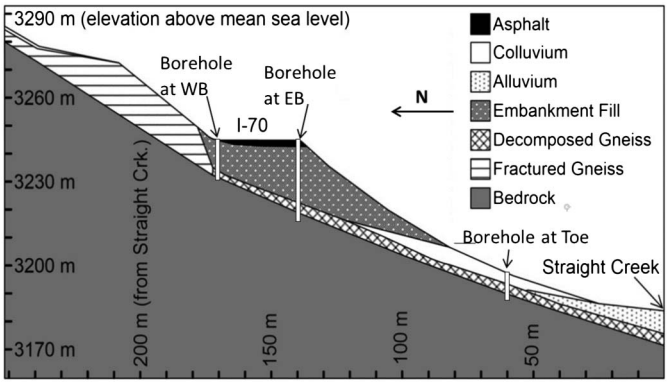

Fig. 2. Transect showing subsurface material distribution along the slide centerline (AA-–^{A} / in Fig. 1).

J. Geotech. Geoenviron. Eng., 2019, 145(9): 05019008

Table 1. Hydromechanical properties of site materials

Material	Soil-water retention properties [van Genuchten (1980) mode] (drying)				Saturated hydraulic conductivity, k_s (m/day)	Soil unit weight, γ (kN/m^3)	Cohesion, c (kPa)	Peak friction angle, φ' (degrees)	Elastic modulus, E (kPa)	Poisson's ratio, v
	θ_r	θ_s	α	n						
Bedrock	0.06	0.34	1.374	1.72	0.001	23	5,638	56	5.3×10^7	0.3
Decomposed gneiss	0.065	0.41	7.5	1.89	1.06	22	25	38	50,000	0.25
Colluvium	0.08	0.33	2.35	2.12	6	20	0	34	50,000	0.25
Alluvium	0.07	0.33	2.35	2.12	3	20	0	30	50,000	0.25
Fractured gneiss	0.06	0.34	1.374	1.72	40	22	1,590	52	1.0×10^7	0.3
Embankment fill	0.08	0.33	1.374	2.12	0.5	21	25	35	30,000	0.25

derived from testing on cores from past drilling (Thunder 2016) or reported by CDOT (Table 1). The bedrock in the slide area is primarily massive dark gneiss, which is relatively impermeable compared with overlying materials. The bedrock surface is generally parallel to the ground surface.

Overlying the competent bedrock is a layer of fractured and weathered material derived from the same dark gneiss, varying in thickness from 1 m to close to 30 m. The degree of weathering increases further down the slope; therefore, this layer was divided into two groups for the conceptual and numerical models. The first group, called fractured gneiss, is found on the slope above the embankment; it presents clean fracture surfaces with little weathering or infill and has high frictional strength and hydraulic conductivity. The second group, called decomposed gneiss, is found underneath the embankment and to the south of it. This material displays a higher degree of weathering, with lower strength and hydraulic conductivity than the fractured gneiss material.

Surficial soil on the slope consists of colluvial deposits with angular, coarse sand to cobble-sized grains derived from the gneiss bedrock. Alluvial soil on the valley floor is more uniform, consisting of rounded sand-sized grains, and was deposited by Straight Creek. Mechanical properties for the two materials are similar, but the hydraulic conductivity of the colluvium is higher due to a lower in situ density caused by depositional processes.

The tunnel-cuttings material used for embankment fill is extremely heterogeneous, including large rock fragments and boulders, construction rubble (such as decomposing timbers from shoring), and more fine-grained material than the surrounding native soils (Robinson & Associates 1971). Hydraulic conductivity of this material is very low due to this fines content. The embankment fill is approximately 14 m thick under the westbound shoulder of I-70, approximately 29 m thick under the eastbound shoulder, and extends approximately 61 m downslope.

Phase I of the investigation included the development of a conceptual model of the seasonal hydrology driving the episodic activation of the landslide (Lu et al. 2013), which consists of seasonal stages (Fig. 3). Stage I is a steady-state condition during the winter with the groundwater table at its lowest level, resting along the surface of the competent bedrock. During this period, snowpack accumulates with essentially no melting or other infiltration occurring. Stage II, corresponding to the spring, is defined by rapid melting of the snowpack; this meltwater begins infiltrating into the upper layers of soil. Subsurface flow is initially perpendicular to the slope during this period because moisture gradients control flow direction more than gravity (simulated pathlines near the slope surface in Fig. 3); as the slope becomes wetter, vertical flow predominates (Lu et al. 2011) (simulated pathlines in the middle of the slope in Fig. 3). Stage III is defined by higher saturation within the hillslope and a slower surface infiltration rate, driven by summertime precipitation instead of snowmelt.

The hydraulic conductivity contrast between the fractured gneiss and competent bedrock layers promotes increased lateral downslope flow along the bedrock interface. The increased lateral flow then encounters the contrast in hydraulic conductivity between the fractured gneiss and embankment material and decomposed gneiss found lower on the slope. Such sharp contrast in hydraulic conductivity could cause a rapid and pronounced elevation in groundwater levels underneath the westbound lanes of the highway; this spike could be both delayed and reduced in scale underneath the eastbound lanes, due to the attenuating effect of the low-hydraulic-conductivity highway embankment fill. The groundwater rise increases positive pore pressures along the failure surface throughout the summer season, reducing effective stress or increasing suction stress and frictional resistance and causing slide activation. During the fall season, precipitation slows or takes the form of snow, and the hillslope drains out and approaches the winter-stage steady state.

Data sources used to analyze slide movement rate include inclinometers and interviews with CDOT employees and contractors. Informal interviews (D. Thomas, personal communication, 2010) with CDOT employees indicate periods of increased movement in 1986 and 1996–1997. Inclinometers have been deployed on this slide at several points within the last 3 decades. Following Kumar & Associates' (1997) report, CDOT installed three inclinometers; they were outranged within 3 years and therefore unable to record further slope movements. In 2008, CDOT installed two more inclinometers, INC2 along the eastbound shoulder and INC3 along the westbound shoulder; these both measured approximately 5 cm of movement perpendicular to the highway within 2 years. In Phase I of the CSM and USGS investigation, two more inclinometers were installed alongside piezometers: INC4 under the westbound shoulder, and INC5 under the eastbound shoulder. Inclinometer data (and some survey monument measurements) indicate more than 5 cm of lateral movement in both 1996 through 1997 and 2008 through 2009.

Precipitation data are obtained from a snow telemetry (SNOTEL) data gathering station at Grizzly Peak (NRCS 2018), approximately 14 km to the southeast of the slide site, which is maintained by the Natural Resource Conservation Service (NRCS) of the US Department of Agriculture (USDA). For the calculation of infiltration amounts in this investigation, as has been done in some previous work (e.g., Osawa et al. 2018), any negative change in snow water equivalent (SWE) is interpreted as snowpack melting and assumed to directly infiltrate (defined as snowmelt infiltration). Any increase in cumulative precipitation occurring when SWE is zero (i.e., no snowpack existed) and temperatures are above freezing is assumed to also directly infiltrate (defined as rainfall infiltration), whereas precipitation occurring on a day with a nonzero SWE is assumed to either add to the snowpack or dissipate as runoff.

There are limitations to the direct applicability of data collected at Grizzly Peak to the slide site; in addition to the distance between

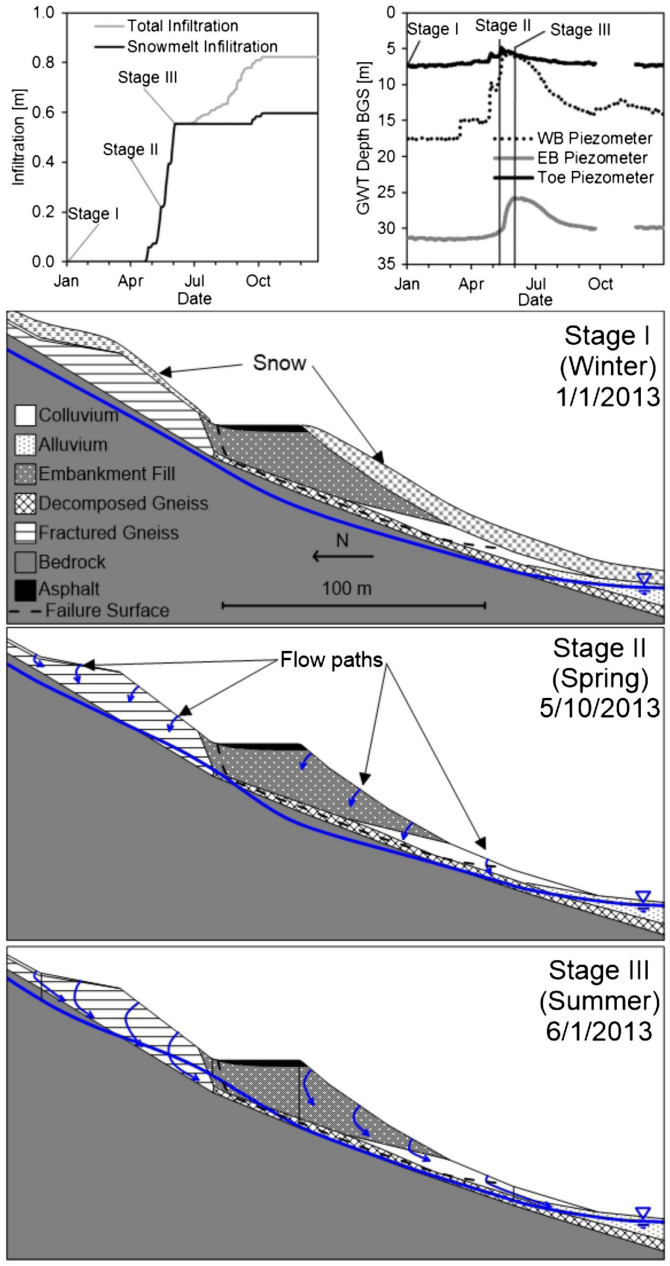

Fig. 3. Conceptual model of seasonal hydrology, linked to infiltration and piezometer data from 2013.

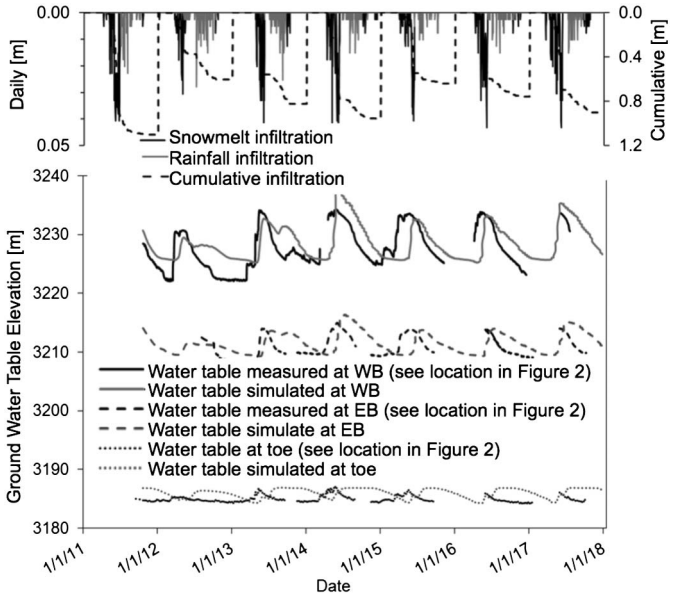

Fig. 4. Measured and simulated groundwater table elevations and infiltration data, 2011–2018.

them, the two locations differ in some important ways. The Grizzly Peak site is topographically flatter, more heavily vegetated, and more removed from roadways than the Straight Creek slide area; it also does not face as directly south. Generally, this has been found to result in a later onset of snowmelt at Grizzly Peak than at the Straight Creek slide. Thunder (2016) found that shifting the infiltration data 2 weeks earlier provided a modeled hydrologic response that better matched the observed response; overall, however, the Grizzly Peak data are thought to provide a reasonably accurate measurement of precipitation conditions at the Straight Creek slide site.

CSM currently maintains eight piezometers distributed over the Straight Creek site; these piezometers record groundwater pressure every 2 h, which is then converted into groundwater depth. Two of these piezometers (WB, under the westbound shoulder of I-70, and Toe, near the slide toe) were installed in 2011, one was installed in 2012 (EB, under the eastbound shoulder of I-70), another in 2016 (North, about 70 m north of the westbound shoulder of I-70), and four were installed in 2017 (to the east and west of the North and WB piezometers).

Data Synthesis and Numerical Analysis

A hydromechanical model is established to synthesize and analyze the site hydrologic and mechanical conditions. All modeling is conducted using HYDRUS 2D version 2.0 (Šimůnek et al. 2011), a finite-element software package capable of modeling groundwater hydrology by solving Richards' equation (Richards 1931), an adaptation of Darcy's Law to transient flow in variably saturated soils. The van Genuchten (1980) Soil Water Characteristic Curve (SWCC) model and Mualem (1976) Hydraulic Conductivity Function (HCF) model are used to parameterize soil hydrologic properties. The Slope Cube module of HYDRUS 2D (Lu et al. 2016) is used for all stress field computation and stability analyses. Slope Cube incorporates Lu et al.'s (2010) unified effective stress theory for variably saturated soils under both compressive pore-water pressure and suction conditions, which allows standard Mohr-Coulomb failure criterion and strength parameters, i.e., cohesion and friction angle (peak), to be used under both saturated and unsaturated conditions. For simplicity, an advanced postfailure or strength-softening analysis technique is not used. Such simplification may result in overestimating the strength of the materials (e.g., Stark and Hussain 2009).

The multiyear water table variation data are used to test the direct use of snowmelt data to inform the infiltration boundary condition with the 2-week shift used by Thunder (2016). This is because the cumulative snow is less than 6 months old, porous, and its hydraulic conductivity is high, and the snowmelt rate seldom exceeds the soil's saturated hydraulic conductivity at the site. The simulation results are shown in Fig. 4, indicating that the direct use of the snowmelt data as infiltration on the slope surface is a good assumption in terms of the prediction of the overall water table variations over the observed years. However, the simulations compare much better with the observed data at the WB piezometer than at EB or Toe piezometers. This is acceptable considering the

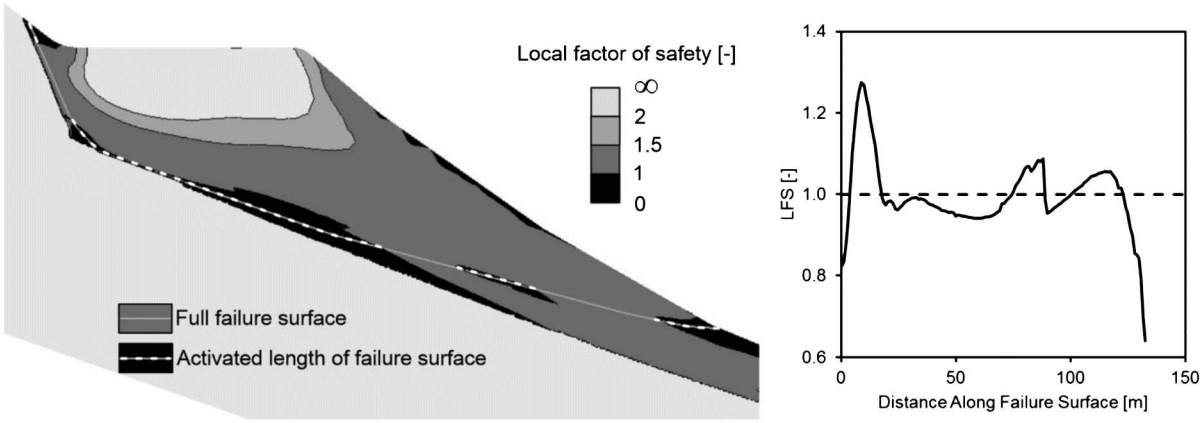

Fig. 5. LFS contour map of embankment at critical state, showing activated length concept and distribution of LFS over the failure surface.

importance of the relation between the buildup of groundwater within the northern slope above the road embankment and landslide activity.

Initial stress field due to gravity as well as the consequent stress changes due to changes in soil suction are computed in the Slope Cube module. A local factor of safety (LFS) method is used for stability calculations (Lu et al. 2012). The LFS method calculates a ratio between resistance and driving stresses at every point in a model domain, leading to a contour of LFS. The concept of an activated length is used to assess the results of LFS analyses, whereby the length along an identified failure surface (derived from LFS contour plots) with LFS < 1 is expressed as a percentage of the full failure surface (Fig. 5). Because the hydraulic conductivity of the embankment material is low and the seasonal patterns of pore-water pressure buildup are similar each year, a higher activated length indicates increased instability. For this model, the critical threshold of activated length is identified by integrating the distribution of LFS over the identified failure surface and finding the activated length at which this integration is equal to zero (Fig. 5). Strength parameters are adjusted so that this critical threshold (identified as 62.5% of the total failure length along the failure surface) is just reached at two points, with the lowest simulated instability corresponding to periods of known pronounced movement (Fig. 6 describing the summers of 1986 and 2009).

Model geometry is based on the transect in Fig. 2, with the north boundary extended 740 m up to the watershed boundary (Fig. 1); this large extent of northern slope is needed to generate the high

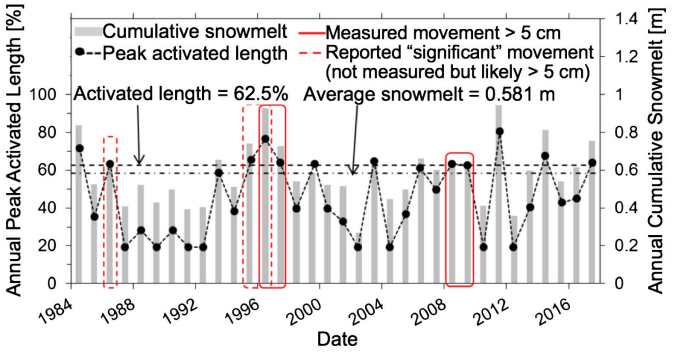

Fig. 6. Annual cumulative snowmelt infiltration, modeled annual peak activated length (measure of maximum instability), and periods of known pronounced movement, 1984–2012.

lateral subsurface flux caused by infiltration over the entire slope up to the drainage divide. The south boundary is also extended 100 m to reduce boundary effects in stress calculations. The mechanical boundary conditions at both the north and south boundaries are no horizontal displacement but free vertical displacement. The mechanical boundary conditions at the bottom are no vertical displacement but free horizontal displacement. Based on site geologic and hydrologic conditions, the hydrologic boundary conditions are set to no flux at (1) the bottom and north boundaries due to the relative low hydraulic conductivity of the bedrock and intact rock, and (2) the highway surface due to the relative impermeable layer of asphalts. A specified flux boundary condition is used at the slope surface to allow applied infiltration for both rainfall and snowmelt precipitation. A constant head is applied at the south boundary to reflect the modulating effect of Straight Creek, which approximately coincides with that boundary. Although the water level of Straight Creek may vary, the annual fluctuation is less than a few feet or a meter. The effect of such change has a minimum effect on the groundwater table variation within the slope, as indicated in the recorded data nearby at the toe of the slope shown in Fig. 4. The Mohr-Coloumb failure criterion is used to represent the shear strength of the slope materials, and the corresponding strength parameters obtained from the previous investigation (Lu et al. 2013) are presented in Table 1. For simplicity, this investigation does not consider the variability of soil properties at the field-scale analysis.

To set initial conditions, a novel approach is used: instead of applying a single constant infiltration rate on the slope surface, an average year of infiltration data is created by distributing the average accumulated infiltration for both spring snowmelt and summer rainfall seasons over the average duration of these seasons. This gives rates of 0.0116 m/day during the snowmelt season, which runs from April 1 to May 21, and 0.00152 m/day during the rainfall season, which runs from May 22 to September 22. No infiltration is applied on the slope during all other periods of the average year. This infiltration cycle is then applied for 60 years, which is found to be sufficient for a steady cyclical state to be reached; this steady cyclical state was defined as one in which, under steady annually cyclical infiltration, peak and minimum pressure heads at the observation nodes do not change between years. This is therefore considered appropriate as a representative initial hydrologic conditions for investigating sensitivity to annual variability in infiltration. All model runs using these initial conditions begin on January 1.

Simulated pressure heads at observation nodes corresponding to piezometer locations are generated using daily SNOTEL

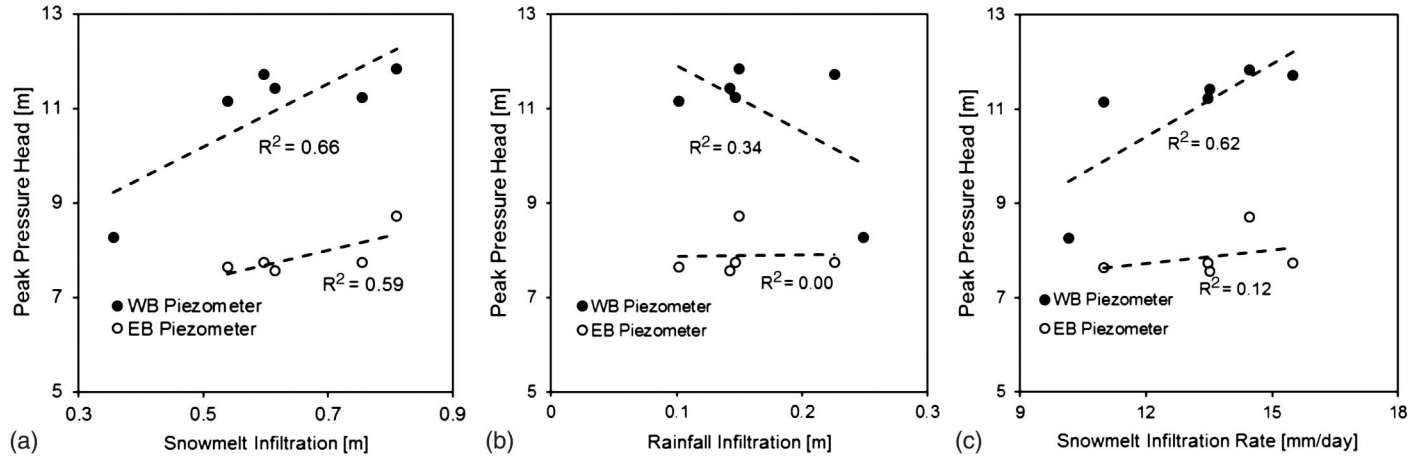

Fig. 7. Correlations between annual peak pressure heads and (a) annual cumulative snowmelt infiltration; (b) annual cumulative rainfall infiltration; and (c) seasonal snowmelt infiltration rate. Both snowmelt characteristics are more strongly and positively correlated with annual peak pressure heads.

infiltration data for the years over which piezometer data are available; soil hydrologic properties and spatial distribution are then calibrated within ranges constrained by the literature, previous laboratory testing programs, and interpretation of borehole logs to match observed piezometer data as closely as possible. Annual peak pressure heads, which are considered the most critical hydrologic result because they directly cause peak instability, generally match piezometer data very well, as shown in Figs. 4 and 6, as do annual minimum pressure heads; the timing of pressure head change does not. Some discrepancy may be explained by differences between the Straight Creek slide site and the SNOTEL station site, which is 14 km away in a different (although similar) watershed, and in a location that is topographically flatter, more heavily forested, and more distant from roadways than the Straight Creek slide. These differences may be sufficient to cause the persistent disparity in timing and occasional disparity in magnitude of groundwater level peaks.

Sensitivity of Slope Stability to Annual Infiltration Characteristics

In every year on record, cumulative snowmelt infiltration is both much greater in magnitude (average of 0.581 m annual cumulative snowmelt infiltration versus 0.190 m annual cumulative rainfall infiltration) and occurs over a much shorter timescale (average duration of 45 days for snowmelt season versus 116 days for rainfall season). This suggests that snowmelt characteristics likely have a larger effect on embankment stability than rainfall. Years of above-average annual cumulative snowmelt infiltration coincide with known periods of pronounced slide movement, and with higher modeled instability (Fig. 6). There are years of above-average annual cumulative snowmelt infiltration and high modeled instability for which pronounced movement is not noted (1984, 1993, 2003, 2006, 2007, and 2011); however, these years all occur during periods without inclinometer or continuous piezometer data. It is possible that little movement occurred despite high infiltration and pore pressures; informal interviews may have simply failed to record pronounced movement during these years, or extensive roadwork in 2011 may also have obscured pronounced movement during that year.

The rate of infiltration may have an effect on instability independent of the depth of cumulative infiltration. For a given depth of cumulative infiltration, a higher rate of infiltration creates higher subsurface flux (for a shorter duration), which exacerbates the pressure head increase at the hydraulic conductivity contrast at the embankment's upslope boundary. This compounding effect of infiltration rate is possibly evident in Fig. 6: 1986, a year of known pronounced movement, had slightly higher than average cumulative annual snowmelt infiltration but had the third highest rate of snowmelt infiltration on record (17.6 mm/day, compared with average and maximum rates of 12.9 and 21.8 mm/day, respectively).

Correlations between annual infiltration characteristics and annual peak pressure heads measured by piezometers strengthen the hypothesis that annual cumulative snowmelt infiltration and rate of snowmelt infiltration are the most important drivers of pressure heads beneath the embankment [and therefore of slide movement (Fig. 7)]. Annual cumulative snowmelt infiltration and rate of snowmelt infiltration both have fairly strong positive correlations with annual peak pressure head at the WB piezometer (under the westbound shoulder), and weaker, less positive correlations with annual peak pressure head at the EB piezometer (under the eastbound shoulder). This is due to the attenuating effect of the low-hydraulic-conductivity materials within and beneath the embankment. As shown in Fig. 7, all rainfall characteristics have very weak or nonexistent correlations with peak pressure heads, confirming that rainfall is essentially unrelated to embankment stability. This is because rainfall infiltration spreads over much longer period of time (May to October) than snowmelt (in a month or so in April).

To study sensitivity to annual cumulative snowmelt and rainfall infiltration using numerical modeling, input data are prepared using five cumulative annual infiltration amounts for each type of infiltration covering the range of observed values (Table 2). All possible combinations of these values for snowmelt and rainfall infiltration result in 25 unique infiltration scenarios for cumulative annual infiltration amounts, which are then distributed over a time period typical for each infiltration scenario, i.e., April 1 to May 21 for snowmelt infiltration and May 22 to September 22 for rainfall infiltration, meaning that the infiltration rate varies. The infiltration data created by distributing a depth of cumulative infiltration over a typical duration are referred to as a generalized year to differentiate it from the use of daily infiltration data calculated directly from SNOTEL data.

The resulting 25 possible combinations of snowmelt and rainfall infiltration are then each modeled, and the resulting activated length (LFS < 1 along typical failure surface) for each combination is used

Table 2. Cumulative infiltration levels used in modeling synthesis

Infiltration characteristic	Level 1 (minimum)	Level 2	Level 3 (average)	Level 4	Level 5 (maximum)
Annual cumulative rainfall (m)	0.102	0.146	0.190	0.268	0.345
Annual cumulative snowmelt (m)	0.267	0.424	0.581	0.767	0.953
Snowmelt infiltration rate (mm/day)	7.7	10.3	12.9	17.4	21.8

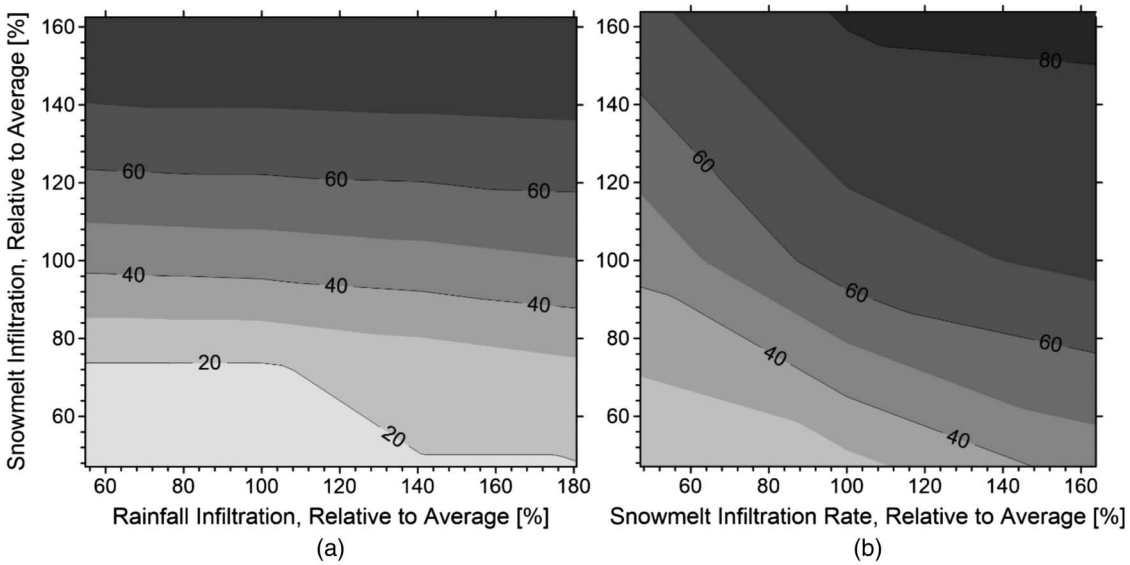

Fig. 8. Contour plots of activated length modeled for various combinations of annual cumulative snowmelt infiltration and (a) rainfall infiltration; or (b) snowmelt infiltration rate.

to produce a contour plot [Fig. 8(a)]. The range of observed annual cumulative snowmelt infiltration can change the activated length by 60% of the full failure surface, whereas the range of observed annual cumulative rainfall infiltration can only change the activated length by 3.7% of the full failure surface (for an average value of annual cumulative snowmelt infiltration). The large activated length of the failure surface due to the snowmelt infiltration is because that snowmelt infiltration occurred in much shorter period of time than the rainfall infiltration; the former occurred in days and the latter occurred over many months. Because rainfall is shown to be relatively unimportant to embankment stability, the effect of infiltration rate is only studied for snowmelt infiltration. The same five levels of annual cumulative snowmelt are modeled at five different levels of snowmelt infiltration rate (Table 2), requiring the duration to vary as well, and the resulting activated length for each combination is used to produce a contour plot [Fig. 8(b)]. For the average value of annual cumulative snowmelt infiltration, the range of observed snowmelt infiltration rate can change activated length by 29% of the full failure surface, substantially more than the maximum effect from rainfall infiltration.

In approximately two-thirds of the years on record, the main snowmelt season is preceded by an early partial snowmelt event. These events involve an average of 0.033 m of snowmelt infiltration, last for 1–2 weeks, and occur up to 2 months earlier than the onset of the main snowmelt season. Small, prewetting events like this have in the past been found to accelerate and increase downslope subsurface flow (Whipkey 1965; Lu and LeCain 2003) by bringing hydraulic conductivity of subsurface materials closer to maximal, saturated values. The simulations were conducted to examine if these aforementioned prewetting events have more significant effects in the high hydraulic conductivity materials in the northern slope than in the low-hydraulic-conductivity materials within and beneath the embankment. If so, these prewetting events could exacerbate seasonally destabilizing pressure head increases by increasing the hydraulic conductivity contrast. However, it is found that early partial snowmelt events actually have a mitigating effect, allowing pressure heads to dissipate more quickly due to increased saturation of the low-hydraulic-conductivity materials. This mitigating effect is not substantial; the greatest decrease in activated length due to early partial snowmelt is about 1%.

Of all the infiltration characteristics studied, annual cumulative snowmelt infiltration is the most important driver of hydrology and instability. Its effect on the activated failure surface length is multiple times greater than that of any other factor. The rate at which snowmelt infiltrates is the second most important factor because it can substantially change activated failure surface length for a given depth of annual cumulative snowmelt infiltration; all other factors studied are essentially negligible. The effect of snowmelt characteristics is dominant because for the particular climate of this site, snowmelt is greater in quantity and rate than rainfall.

Sensitivity of Slope Stability to Infiltration in Preceding Year

The effect of antecedent soil-moisture conditions on slope stability during infiltration has been firmly established; long-term (seasonal to annual scale) conditions have also been identified as particularly important (Campbell 1975). Periods of known pronounced movement of the Straight Creek slide tend to coincide not only with years

of above-average annual cumulative snowmelt infiltration, but also with periods of such years occurring consecutively (Fig. 6). This suggests that presnowmelt groundwater levels may be affected by infiltration in the previous year; a year of above-average annual cumulative snowmelt infiltration may produce increased soil moisture that does not drain out to the same state as after a year of average or below-average annual cumulative snowmelt infiltration. This increase in antecedent soil-moisture conditions or groundwater level, referred to as a carryover effect in soil moisture, may amplify the seasonal increase in pressure heads following snowmelt infiltration, as reported in some other studies (e.g., Wieczorek and Glade 2005).

The period for which piezometer data are available is too short to conduct a rigorous analysis of this possible carryover effect. To expand the number of years available for analysis, a different measure of or proxy for groundwater levels is necessary; data from USGS Stream Gauge 09051050 (USGS 2018), which is located 7.8 km to the west-southwest (downstream along Straight Creek) from the slide site, are available from 1987 onward, providing a larger data set for comparison with infiltration data. Base flow, which is generated by and therefore a proxy for groundwater, can be calculated from the stream gauge total flow data using a single-parameter digital filter based on the work of Lyne and Hollick (1979), Nathan and McMahon (1990), Arnold and Allen (1999), and Arnold et al. (2000), as incorporated into the Web-Based Hydrograph Analysis Tool (WHAT) created by Purdue University's College of Engineering (Lim et al. 2005). The average subsequent winter base flow and minimum subsequent winter base flow can then be correlated to annual cumulative snowmelt infiltration; winter is defined as December 1 through March 31 for this analysis. There is in fact a positive correlation between the snowmelt infiltration in a given year and the base flow during the following winter (Fig. 9). This correlation cannot completely explain variation in wintertime base flow, but could explain much of the variation. Some discrepancy may be explained by the distance of both the stream gauge and SNOTEL site from the slide, and by the drainage area of the stream gauge, which is much larger (47.7 versus 0.3 kmkm^{22}) and more varied than the slide site watershed. If the assumption that changes in base flow correspond to changes in groundwater level is valid, then the proposed carryover effect seems likely to exist to some degree.

The effect of infiltration history is modeled using daily infiltration data for 2009, 2008, 2001, and 2002; annual totals for these years and the 1984–2017 averages are presented in Table 3. The year 2009 had slightly higher than average annual cumulative snowmelt infiltration, one of the lowest values for a year of known pronounced movement, and was preceded by a year (2008) of higher annual cumulative snowmelt, which resulted in an activated length of 62.5%. Because this is the lowest annual peak activated length for any year of known pronounced movement (also simulated for 1986, another year of known pronounced movement and slightly higher-than-average annual cumulative snowmelt infiltration), it is considered a threshold for elevated instability. By modeling 2009 as preceded by years of lower-than-average annual cumulative snowmelt infiltration (2001 and 2002), the effect of infiltration history on the development of instability is demonstrated. When preceded by 2001 or 2002, the annual peak activated length simulated in 2009 is reduced to 57.9% or 52.0%, respectively (Fig. 10). The reduction in peak activated length by up to 10.5% of the full failure surface is potentially enough to substantially reduce or even eliminate movement in 2009 (Fig. 6); this effect from the preceding year's infiltration is greater than that of annual cumulative rainfall infiltration for the Straight Creek site.

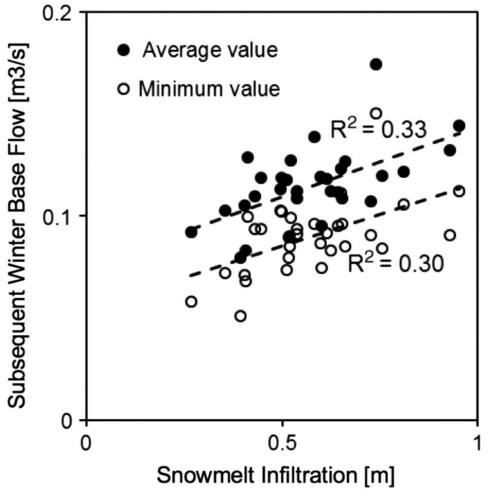

Fig. 9. Correlations between infiltration and base flow in the subsequent winter season.

Table 3. Infiltration characteristics for 2009, 2008, 2001, and 2002

Year	Snowmelt infiltration (m)	Rainfall infiltration (m)	Total infiltration (m)
Average	0.581	0.190	0.771
2009	0.625	0.117	0.742
2008	0.643	0.203	0.846
2001	0.516	0.163	0.678
2002	0.267	0.208	0.475

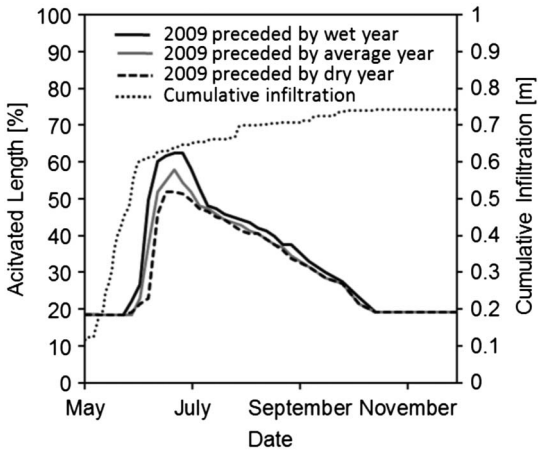

Fig. 10. Activated length time series for 2009, modeled as preceded by different years.

The duration of the peak in activated length is also affected by the preceding year; for a year in which peak activated length will exceed 62.5% regardless of infiltration in the previous year, the period of time for which it will exceed this threshold will be responsive to this infiltration history. It is reasonable to expect that a longer period above this threshold will result in greater magnitude of slide movement. It was found that infiltration during the preceding year has a moderate but clear carryover effect on the hydrology and stability of the Straight Creek slide. Years of above-average annual cumulative infiltration increase groundwater levels at the onset of

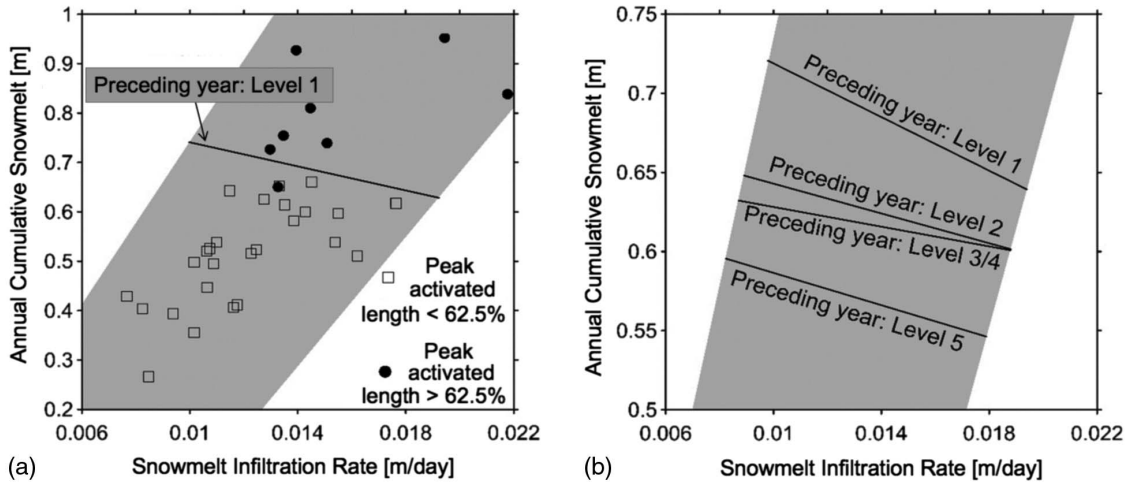

Fig. 11. (a) Predictive framework development; and (b) final thresholds. Shaded area indicates region of observed data.

snowmelt in the following year, increasing the resultant peak pressure heads. Meanwhile, years of below-average annual cumulative infiltration have the opposite effect. The ability of the numerical model to simulate the importance of antecedent infiltration also corroborates the validity of the identified threshold of the failure length for landslide reactivation.

Development of a Predictive Framework for Instability Threshold

The preceding sections demonstrate that annual cumulative snowmelt infiltration, rate of snowmelt infiltration, and annual cumulative infiltration in the preceding year are all important factors behind instability in a given year. This suggests the possibility of developing thresholds of combinations of these factors, above which pronounced movement is likely. These thresholds could aid CDOT in allocating resources to monitor for and rapidly address issues caused by increased movement.

To set these thresholds, each year of available SNOTEL data (1984 through 2017) is modeled separately, preceded by years of different annual cumulative snowmelt infiltration. These preceding years were created by multiplying daily infiltration rates for a year of average annual cumulative snowmelt infiltration (1999) by a factor to match annual cumulative snowmelt infiltration to the levels specified in Table 2. Level 1 therefore represents a preceding year of minimal annual cumulative snowmelt infiltration, Level 5 a preceding year of maximal annual cumulative snowmelt infiltration, and Levels 2 through 4 distributed evenly within the observed range. The resulting activated length is then compared with the minimum activated length corresponding to pronounced movement, which was set equal to the activated length modeled for 1986 and 2009 when all years were modeled sequentially (as in Fig. 6). This is the lowest activated length modeled for a year of known pronounced movement. The threshold for infiltration that will likely cause this activated length can then be drawn between model cases that did or did not exceed it [Fig. 11(a)], disregarding outliers as needed. These thresholds for each level of annual cumulative snowmelt infiltration in the preceding year can then be combined [Fig. 11(b)].

Predicting snowmelt rate is not as straightforward as predicting annual cumulative snowmelt infiltration, which can be accurately estimated from SWE values preceding the main snowmelt season (which typically begins in April or early May). There are no clear correlations between temperature and snowmelt rate that apply across all years, even controlling for annual cumulative snowmelt infiltration. However, there are 11 identifiable cases of years with annual cumulative snowmelt infiltration within 5 mm of each other, nine of which have an identifiable difference in snowmelt rate. Of the nine cases, eight can be explained by the onset of snowmelt, and nine can be explained by the average temperature during the 45 days following the onset of snowmelt. Later onset, closer to early May than mid-April, coincides with high average temperatures in the subsequent snowmelt season and a faster snowmelt rate. These observations can be used as rough guides for estimating snowmelt rate, similar to the approach proposed by Chleborad (1998).

Quantifying the Straight Creek slide's sensitivity to infiltration characteristics may therefore prove to not only add to the general body of knowledge related to infiltration-induced landslides, but to provide practical benefits to CDOT in managing the risks of this slide. Through the use of this predictive framework, it may be possible to anticipate pronounced movement based on infiltration in the previous year and predicted annual cumulative snowmelt infiltration and snowmelt infiltration rate in the current year. This also represents a contribution toward developing hydrometeorological thresholds based on the physical processes driving landslide initiation or reactivation (Bogaard and Greco 2018; Mirus et al. 2018a, b; Thomas et al. 2018).

Summary and Conclusions

Infiltration-induced landslides are common hazards around the world, with frequent and substantial fatalities and economic losses. They are triggered by changes in subsurface hydrologic conditions during infiltration; it is increasingly acknowledged that this can include changes in matric suction in the unsaturated zone, not just increased positive pore pressures in the saturated zone (Lu and Godt 2008; Godt et al. 2012, 2009). Anthropogenic global climate change is widely understood to increase the severity and frequency of intense precipitation events in at least some regions of the world (Trenberth 2011), which can be expected to increase the occurrence and impact of infiltration-induced landslides. Understanding the triggering mechanisms of these slides and developing science-based best practices for remediating them will therefore only increase in urgency in the coming decades.

Since 2010, CSM has conducted a continuous multiyear investigation of the infiltration-induced Straight Creek landslide in

partnership with CDOT and USGS-LHP. This investigation has provided valuable insights into the particular subsurface stratigraphy and watershed hydrology that have led to instability at this site for 4.5 decades, while also adding to the body of general knowledge on infiltration-induced landslides and the effects of changes in the unsaturated zone on slope stability. This paper presents several of the findings of the case study, which seeks to use LFS methodology to study the spatial-temporal evolution of slope failure and characterize the slide's sensitivity to single-year and multiyear variability in infiltration. The following conclusions can be drawn:

- Instability at this site is directly triggered by an abrupt dramatic seasonal increase in pore pressure beneath the embankment, which is caused by the rapid infiltration of snowmelt.
- Of the infiltration characteristics studied, annual cumulative snowmelt infiltration is by far the most important single-year factor in the level of slide activation and is likely sufficient to determine whether or not the slide will move and by how much in a given year.
- The rate at which snowmelt occurs also has a substantial effect on stability, although less so than the total amount of snowmelt. A faster rate of snowmelt exacerbates the seasonal increase in pressure head beneath the embankment, which is the cause for instability. All other single-year factors, such as summer season rainfall infiltration, are essentially negligible in comparison with the cumulative annual snowmelt and snowmelt rate.
- Slope stability can be affected by infiltration in the previous year. Consecutive years of high infiltration can have a compounding effect, increasing the magnitude of seasonal pressure head rise and result in less stability than single, isolated years of high infiltration. Likewise, consecutive years of low infiltration can suppress groundwater response to infiltration and increase slope stability in subsequent years.

The case study illustrates that the effects of infiltration characteristics, namely annual snowpack accumulation, forecasted snowmelt rate, and the previous year's snowmelt, can be used to form tools for predicting increased movement of the Straight Creek slide in a given year. This method of developing instability threshold may be applied to other sites once the physical processes underlying the evolution of instability are understood.

Acknowledgments

This project is supported through grants from Colorado Department of Transportation (CDOT SAP No. 411013042) to the second and fourth authors and National Science Foundation (CMMI No. 1561764) to the second author and are greatly appreciated. In-kind support for partial field instrumentation from the Geologic Hazards Science Center of the US Geological Survey is greatly appreciated. Numerous discussions on the evolving geotechnical challenges of the site with David Thomas and Aziz Khan of CDOT are insightful and instrumental in the course of this case study. Matt Thomas (USGS) provided some constructive suggestions for improving an earlier version of this manuscript. Data are available through contacting the corresponding author. Any use of trade, firm, or product names is for descriptive purposes only and does not imply endorsement by the US Government.

References

Arnold, J., and P. Allen. 1999. "Automated methods for estimating baseflow and ground water recharge from streamflow records." *J. Am. Water Resour. Assoc.* 35 (2): 411–424. https://doi.org/10.1111/j.1752-1688.1999.tb03599.x.

Arnold, J. G., R. S. Muttiah, R. Srinivasan, and P. M. Allen. 2000. "Regional estimation of baseflow and groundwater recharge in the Upper Mississippi River Basin." *J. Hydrol.* 227 (1–4): 21–40.

Bogaard, T., and R. Greco. 2018. "Invited perspectives: A hydrological look to precipitation intensity duration thresholds for landslide initiation: Proposing hydro-meteorological thresholds." *Nat. Hazard. Earth Syst. Sci.* 18 (1): 31–39. https://doi.org/10.5194/nhess-18-31-2018.

Campbell, R. H. 1975. *Soil slip, debris flows, and rainstorms in the Santa Monica Mountains and vicinity, southern California*. Professional Paper No. 851. Washington, DC: USGS, US Dept. of the Interior.

Chleborad, A. F. 1998. *Use of air temperature to anticipate the onset of snowmelt season landslides*. Open File Rep. No. 98-124. Washington, DC: USGS.

Godt, J., B. Sener-Kaya, N. Lu, and R. Baum. 2012. "Stability of infinite slopes under transient partially saturated seepage conditions." *Water Resour. Res.* 48 (5). https://doi.org/10.1029/2011WR011408.

Godt, J. W., R. Baum, and N. Lu. 2009. "Can landslides occur under unsaturated soil conditions?" *Geophys. Res. Lett.* 36: L02403. https://doi/org/10.1029/2008GL035996.

Kumar & Associates. 1997. *Progress report of geological and geotechnical data acquisition, embankment slope instability study, Straight Creek, Interstate-70 west of Eisenhower Tunnel, Summit County, Colorado*. Denver: Colorado Dept. of Transportation.

Lim, K., B. Engel, Z. Tang, J. Choi, K. Kim, S. Muthukrishnan, and D. Tripathy. 2005. "Automated web GIS based hydrograph tool, WHAT." *J. Am. Water Resour. Assoc.* 41 (6): 1407–1416. https://doi.org/10.1111/j.1752-1688.2005.tb03808.x.

Lovering, T. S. 1935. Vol. 178 of *Geology and ore deposits of the Montezuma Quadrangle*. Pueblo, CO: US Government Printing Office.

Lu, N., and J. Godt. 2008. "Infinite slope stability under steady unsaturated seepage conditions." *Water Resour. Res.* 44 (11). https://doi.org/10.1029/2008WR006976.

Lu, N., and J. Godt. 2013. *Hillslope hydrology and stability*. Cambridge, UK: Cambridge University Press.

Lu, N., J. W. Godt, and D. T. Wu. 2010. "A closed-form equation for effective stress in unsaturated soil." *Water Resour. Res.* 46 (5). https://doi.org/10.1029/2009WR008646.

Lu, N., and G. LeCain. 2003. "The use of temperature data to estimate infiltration flux beneath a desert wash." *J. Geotech. Geoenviron. Eng.* 129 (7): 665–668.

Lu, N., B. Sener, and J. Godt. 2011. "Direction of unsaturated flow in a homogeneous and isotropic hillslope." *Water Resour. Res.* 47 (2). https://doi.org/10.1029/2010WR010003.

Lu, N., B. Sener, A. Wayllace, and J. Godt. 2012. "Analysis of rainfall-induced slope instability using a field of local factor of safety." *Water Resour. Res.* 48 (9). https://doi.org/10.1029/2012WR011830.

Lu, N., and A. Wayllace. 2011. *In-situ monitoring of infiltration-induced instability of I-70 embankment west of the Eisenhower-Johnson Memorial Tunnels*. Golden, CO: Colorado School of Mines.

Lu, N., A. Wayllace, and G. Formetta. 2016. *The slope cube module for HYDRUS (2D): Simulating slope stress and stability in variably-saturated hillslopes, technical manual, version 1.0*. Madison, WI: Soil Water Retention LLC.

Lu, N., A. Wayllace, and S. Oh. 2013. "Infiltration-induced seasonally reactivated instability of a highway embankment near the Eisenhower Tunnel, Colorado, USA." *Eng. Geol.* 162: 22–32. https://doi.org/10.1016/j.enggeo.2013.05.002.

Lyne, V., and M. Hollick. 1979. "Stochastic time-variable rainfall-runoff modeling." In *Proc., Resources Symp., National Committee on Hydrology and Water Resources*, 89–92. Perth, Australia: Institute of Engineering.

Mirus, B. B., R. E. Becker, R. L. Baum, and J. B. Smith. 2018a. "Integrating real-time subsurface hydrologic monitoring with empirical rainfall thresholds to improve landslide early warning." *Landslides* 15 (10): 1909–1919. https://doi.org/10.1007/s10346-018-0995-z.

Mirus, B. B., M. D. Morphew, and J. B. Smith. 2018b. "Developing hydro-meteorological thresholds for shallow landslide initiation and early warning." *Water* 10 (9): 1274. https://doi.org/10.3390/w10091274.

Mualem, Y. 1976. "A new model for predicting the hydraulic conductivity of unsaturated porous media." *Water Resour. Res.* 12 (3): 513–522.
Nathan, R., and T. McMahon. 1990. "Evaluation of automated techniques for base flow and recession analyses." *Water Resour. Res.* 26 (7): 1465–1473.
NRCS (Natural Resources Conservation Service). 2018. *Colorado SNOTEL sites*. Colorado SNOTEL Site Grizzly Peak (505). Portland, OR: US Dept. of Agriculture, Natural Resources Conservation Service.
Osawa, H., Y. Matsushi, S. Matsuura, T. Okamoto, T. Shibasaki, and H. Hirashima. 2018. "Seasonal transition of hydrological processes in a slow-moving landslide in a snowy region." *Hydrol. Processes* 32 (17): 2695–2707.
Richards, L. A. 1931. "Capillary conduction of liquids through porous mediums." *Physics* 1 (5): 318–333.
Robinson & Associates. 1971. *The geologic investigation of the Straight Creek landslides*. Denver: Colorado Dept. of Highways.
Sidle, R., and H. Ochiai. 2006. *Landslides: Processes, prediction, and land use*. Washington, DC: American Geophysical Union.
Šimůnek, J., M. Th. van Genuchten, and M. Šejna. 2011. *The HYDRUS software package for simulating two- and three-dimensional movement of water, heat, and multiple solutes in variably-saturated media, technical manual, version 2.0*. Vinohrady, Czechia: PC Progress SRO.
Stark, T. D., and M. Hussain. 2009. "Shear strength in preexisting landslides." *J. Geotech. Geoenviron. Eng.* 136 (7): 957–962. https://doi.org/10.1061/(ASCE)GT.1943-5606.0000308.
Thomas, M. A., B. B. Mirus, and B. D. Collins. 2018. "Identifying physics-based thresholds for rainfallinduced landsliding." *Geophys. Res. Lett.* 45 (18): 9651–9661.
Thunder, B. 2016. "The hydromechanical analysis of an infiltration-induced landslide along I-70 in Summit County, CO." Master's thesis, Civil and Environmental Engineering, Colorado School of Mines.
Trenberth, K. 2011. "Changes in precipitation with climate change." *Clim. Res.* 47 (1–2): 123–138. https://doi.org/10.3354/cr00953.
USGS. 2018. *USGS Current Conditions for the Nation: USGS 09051050 Straight Creek below Laskey Gulch near Dillon, CO*. Dillon, CO: National Water Information System, USGS, US Dept. of the Interior.
van Genuchten, M. T. 1980. "A closed form equation for predicting the hydraulic conductivity of unsaturated soils." *Soil Sci. Soc. Am. J.* 44 (5): 892–898. https://doi.org/10.2136/sssaj1980.03615995004400050002x.
Wayllace, A., N. Lu, S. Oh, and D. Thomas. 2012. "Perennial infiltration-induced instability of Interstate 70 embankment west of the Eisenhower/Johnson Memorial Tunnels." In *Proc., GeoCongress 2012 Annual Conf.* Reston, VA: ASCE.
Whipkey, R. 1965. "Storm runoff from forested catchments by subsurface routes." *Bulletin*. Forest Service, USDA.
Wieczorek, G. F., and T. Glade. 2005. "Climatic factors influencing occurrence of debris flows." In *Debris-flow hazards and related phenomena*, 325–362. Berlin: Springer.